Cell Reports Medicine, Volume *5*

Supplemental information

Intervention with metabolites emulating endogenous cell transitions accelerates muscle regeneration in young and aged mice

Reyna Hernandez-Benitez, Chao Wang, Lei Shi, Yasuo Ouchi, Cuiqing Zhong, Tomoaki Hishida, Hsin-Kai Liao, Eric A. Magill, Sebastian Memczak, Rupa D. Soligalla, Chiara Fresia, Fumiyuki Hatanaka, Veronica Lamas, Isabel Guillen, Sanjeeb Sahu, Mako Yamamoto, Yanjiao Shao, Alain Aguirre-Vazquez, Estrella Nuñez Delicado, Pedro Guillen, Concepcion Rodriguez Esteban, Jing Qu, Pradeep Reddy, Steve Horvath, Guang-Hui Liu, Pierre Magistretti, and Juan Carlos Izpisua Belmonte

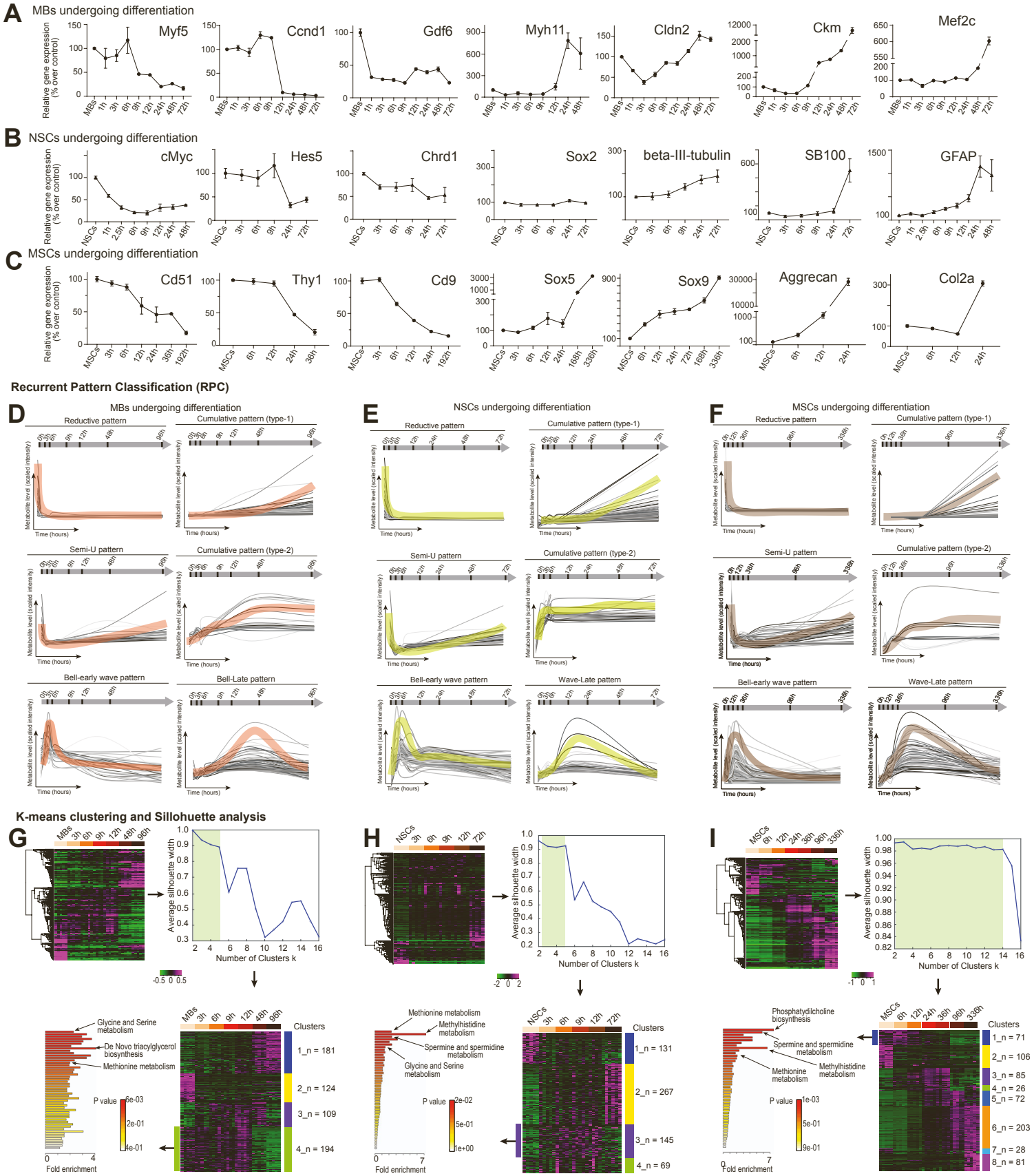

Fig. S1. Comparison of the transitional populations differentiated from MBs, MSCs, and NSCs.
(**A-C**) Reference genes selected to track the transition profile during differentiation of MBs towards myofibers in (A), NSCs towards astrocytes in (B), and MSCs towards chondrocytes (C), represented as percentage over time zero (time 0h= MB-, NSC-, or MSC-steady-state). Total mRNA levels were detected by rtPCR. Expression normalized with the geometric mean of at least two housekeeping genes (from Actb, Gapdh, and Nat1) and then normalized vs. control condition (time=0h). Represented the means ± SEM, n ≥ 3.
(**D-F**) Schematic representation of the abundance patterns of individual metabolites over time. Patterns observed by plotting in a continuous scale of time the mean abundance of each metabolite and then grouped according to the similarity of its behavior on the transitional populations differentiated from MBs in (D), NSCs in (E), and MSCs in (F). Full disclosure of patterns and the algorithms to derive them, in Dataset S1. Gray lines in the background represent each, one metabolite. Colored over line, an illustrative trend. The raw mean values from each metabolite (each gray line) are from n=5.
(**G-I**) Metabolomic analyses in MBs (G), NSCs (H), and MSCs (I). On each panel, hierarchical clustering analysis (HCA) of the fingerprint by time in the transitional populations differentiated from each multipotent stem cells (top left). Following the black arrows, on the side of each HCA, the respective Silhouette analysis (top right; green area indicates predicted appropriate number of clusters), which determines the k-means clustering analysis (bottom right). On the bottom-left panel, the enrichment analysis of selected cluster. Experiments shown are from n=5 biological replicates per cell lineage. Related to Figure 1.

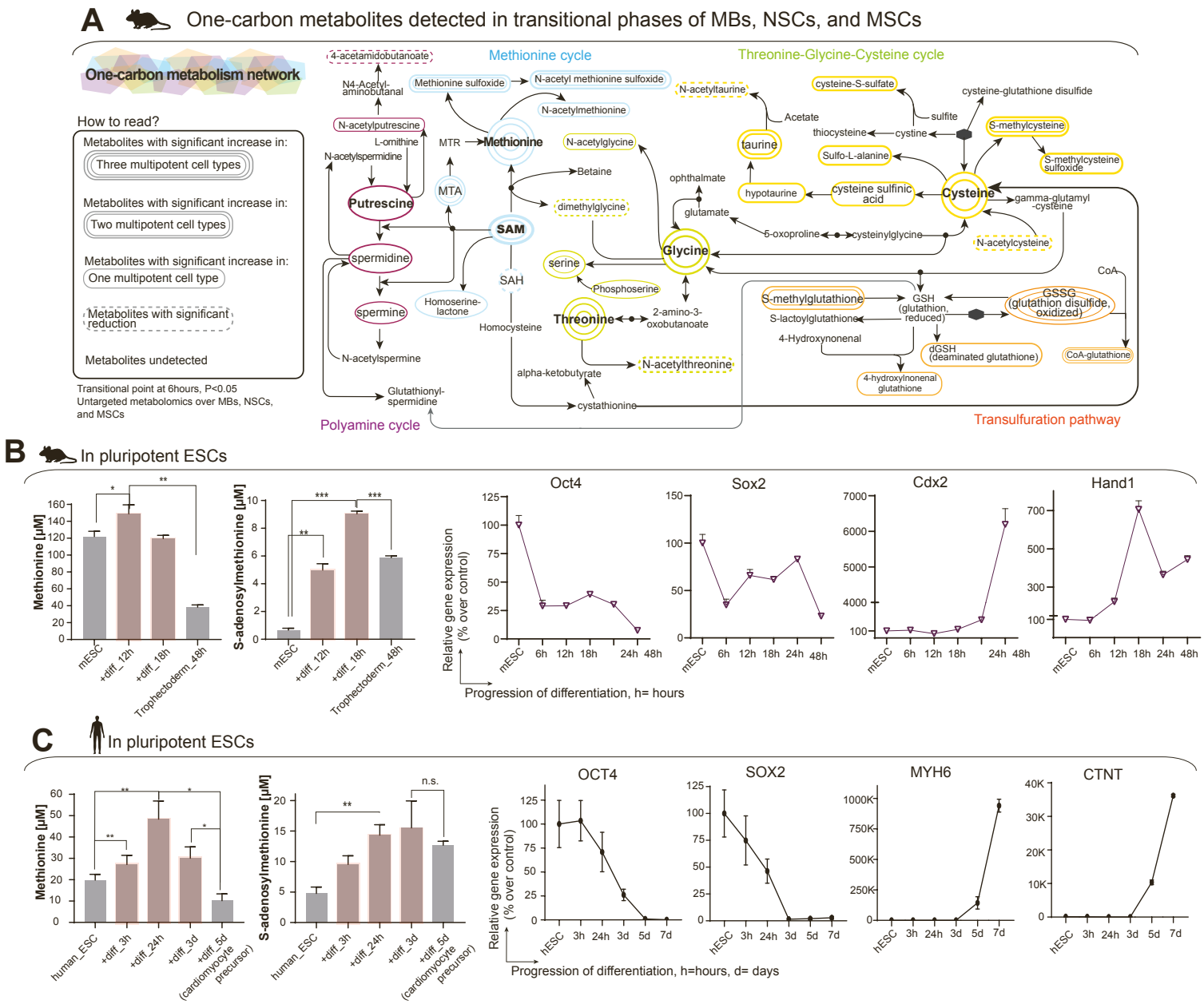

Fig. S2. Common metabolites appear as a wave at the onset of cell identity changes of pluripotent and multipotent cells from mouse and human.

(**A**) Representation of the increase identified in the relative levels of metabolites in three different cell populations derived from MBs, NSCs, and MSCs. Names circled represent metabolites that increase significantly at 6 hours after inducing their differentiation (P<0.05). One, two, or three circles denote significant increases in one, two, or the three cell types, respectively. Dotted circles enclose metabolites that only increase in one cell type, while the other two showed a negative trend. For specific characterization per cell type and times, see Tables S2-S4. Experiments shown are from n=5 replicates per cell type.

(**B**) Quantification of methionine and S-adenosylmethionine (SAM) levels in early states after inducing differentiation of human ESCs to cardiomyocytes; n=3 technical replicates, significantly different at *P<0.05, **P<0.01 (paired t-test). On the right side, as reference for the selection of times, the gene expression of 2-ESC-markers (OCT4 and SOX2) and 2-cardiomyocyte-markers (MYH6, CTNT) measured by rtPCR; where gene expression was normalized to the mean of GAPDH as housekeeping gene, and then normalized vs. control condition (time=0h). Represented the means ± SEM, n = 3.

(**C**) Quantification of methionine and S-adenosylmethionine (SAM) levels in early states after inducing differentiation of mouse ESCs to trophectoderm (cell line Zhbtc4); n=4 technical replicates, significantly different at *P<0.05, **P<0.01 (paired t-test). On the right side, as reference for the selection of times, the gene expression of 2-ESC-markers (Oct4 and Sox2) and 2-trophectoderm-markers (Cdx2 and Hand1) measured by rtPCR; where gene expression was normalized to the mean of Nat1 as housekeeping gene, and then normalized vs. control condition (time=0h). Represented the means ± SEM, n=3.

Means ± SEM, statistically different from controls at **P<0.01, ***P<0.001, and n ≥ 3, where dots represent independent values.
Related to Figure 1.

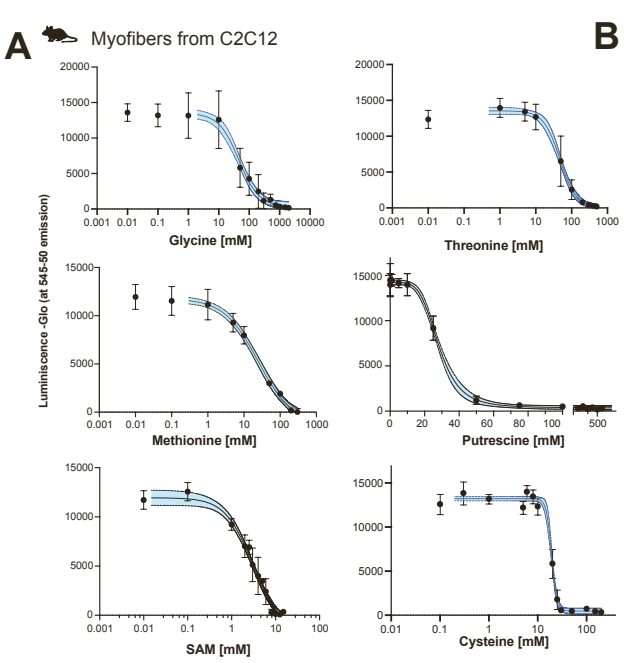

B

Primary Astrocytes

Metabolite: Glycine						
Condition:	*Control*	*0.025mM*	*0.25mM*	*2.5mM*	*5mM*	*10mM*
Gfap relative expression over control	100 ± 4.56	70.19 ± 2.56	68.03 ± 3.65	81.87 ± 6.26	75.96 ± 6.97	73.53 ± 3.16
Metabolite: Methionine						
Condition:	*Control*	*0.025mM*	*0.25mM*	*2.5mM*	*5mM*	*10mM*
Gfap relative expression over control	100 ± 2.55	124.22 ± 4.39	105.73 ± 4.73	113.17 ± 12.7	114.89 ± 18.72	117.36 ± 5.9
Metabolite: Putrescine						
Condition:	*Control*	*0.025mM*	*0.25mM*	*2.5mM*	*5mM*	*10mM*
Gfap relative expression over control	100 ± 13.14	46.66 ± 1.44	57.03 ± 5.99	48.99 ± 2.27	51.79 ± 4.79	☠ LETHAL
Metabolite: Threonine						
Condition:	*Control*	*0.025mM*	*0.25mM*	*2.5mM*	*5mM*	*10mM*
Gfap relative expression over control	100 ± 9.62	22.78 ± 3.78	26..71 ± 2.41	25.13 ± 0.2	22.31 ± 0.08	25.32 ± 0.13
Metabolite: Cysteine						
Condition:	*Control*	*0.025mM*	*0.25mM*	*2.5mM*	*5mM*	*10mM*
Gfap relative expression over control	100 ± 5.85	62.89 ± 2.79	78.8 ± 3.05	127.91 ± 2.53	190.68 ± 7.32	227.6 ± 11.27
Metabolite: SAM						
Condition:	*Control*	*0.1mM*	*0.25mM*	*0.5mM*	*2.5mM*	*10mM*
Gfap relative expression over control	100 ± 6.29	30.95 ± 2.79	27.18 ± 1.48	21.46 ± 1.45	☠ LETHAL	☠ LETHAL
No metabolite, but bFGF						
Condition:	*Control*	*1ng/mL*	*5ng/mL*	*10ng/mL*	*20ng/mL*	
Gfap relative expression over control	100 ± 7.17	267.5 ± 6.5	163.5 ± 10.5	89.0 ± 8.0	64.33 ± 6.69	
No metabolite (BM)						
Condition:	*Control*	*Base Medium (BM)*				
Gfap relative expression over control	100 ± 4.09	82.64 ± 10.04				

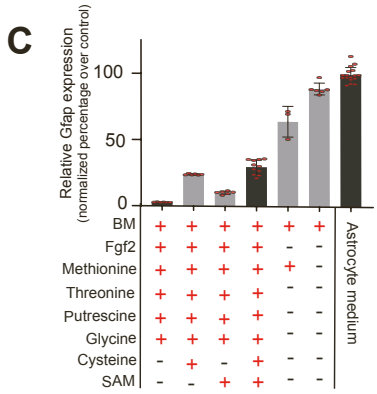

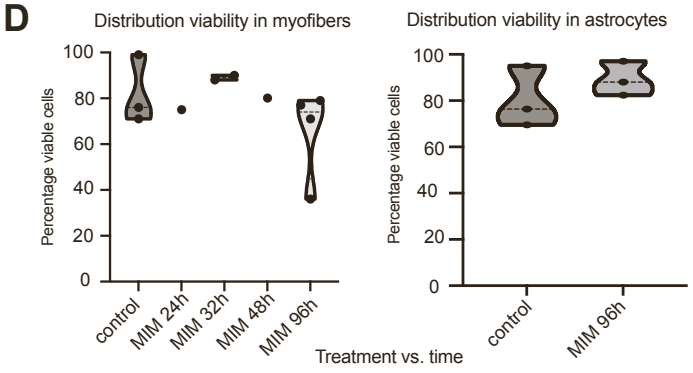

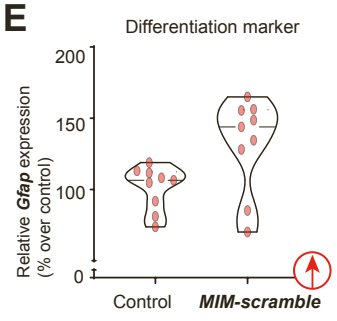

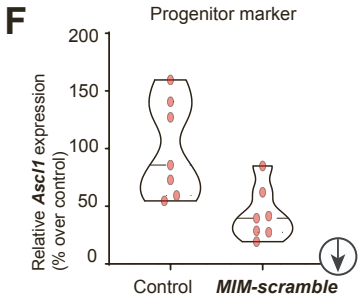

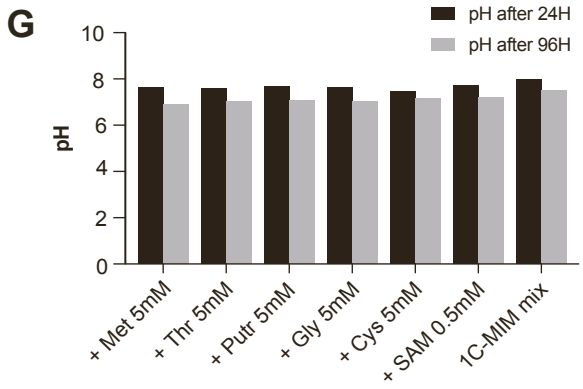

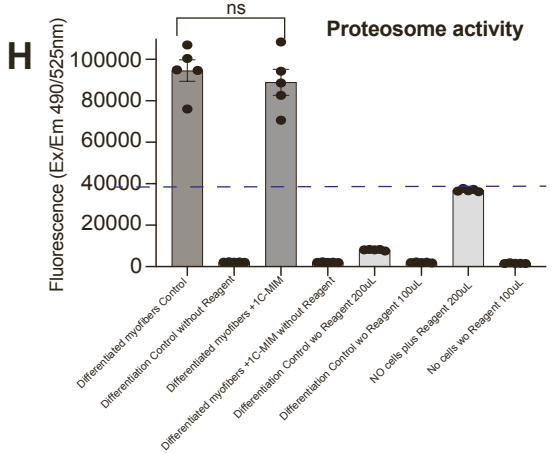

Fig. S3. Standardizations on the supplementation with 1C-metabolites and phenotype changes on differentiated cells.
(**A**) Effect dose-response of individual metabolites over myofibers in vitro, where cell viability is evaluated by the relative quantification of ATP present by a luminescent assay, as an indicator of metabolically active cells.
(**B**) Effect dose-response over the astrocytic phenotype evaluated by levels of expression of the glial marker GFAP; the expression was normalized with the geometric mean of at least two housekeeping genes (from Actb, Gapdh, and Nat1) and then normalized vs. control condition. Dots represent each value ($n \geq 5$), and bars the mean ± SEM.
(**C**) Comparison of 1C-MIM of 6 metabolites (MIM6) versus the elimination of SAM (component lethal at high concentrations) and (or) cysteine (component with higher susceptibility to oxidation), see details in methods. The cocktail without SAM and without cysteine represents the 1C-MIM4 with 4-metabolites. Standardizations were done in mouse astrocytes. Note that the combination without SAM or cysteine achieved more inhibition of the Gfap-marker; thus, both combinations were tested, as seem to be dependent on the cell type.
(**D**) Quantification of viable cells by trypan blue exclusion on myofibers (left panel) and astrocytes (right panel).
(**E**) Evaluation of the effect of a scrambled mixture of metabolites not related to 1C-metabolism. This includes arginine, creatine, fructose, histidine, leucine, and valine; metabolites were added at 5mM (i.e., with similar concentrations than 1C-MIM). Note that scramble-cocktail did not lower Gfap-differentiation-marker neither potentiated the Ascl1-progenitor marker (opposite effect to the observed with 1C-MIM).
(**G**) pH measurements of myoblast in culture in the presence of indicated metabolites (individually or in combination) for 24 or 96 hours.
(**H**) Relative levels of proteosome activation in myofiber cultures supplemented with 1C-MIM, where differences compared with control are significant at **P<0.001 or ***P<0.0001.).
Dots represent each value ($n \geq 5$), and bars the mean ± SEM. Related to Figure 2.

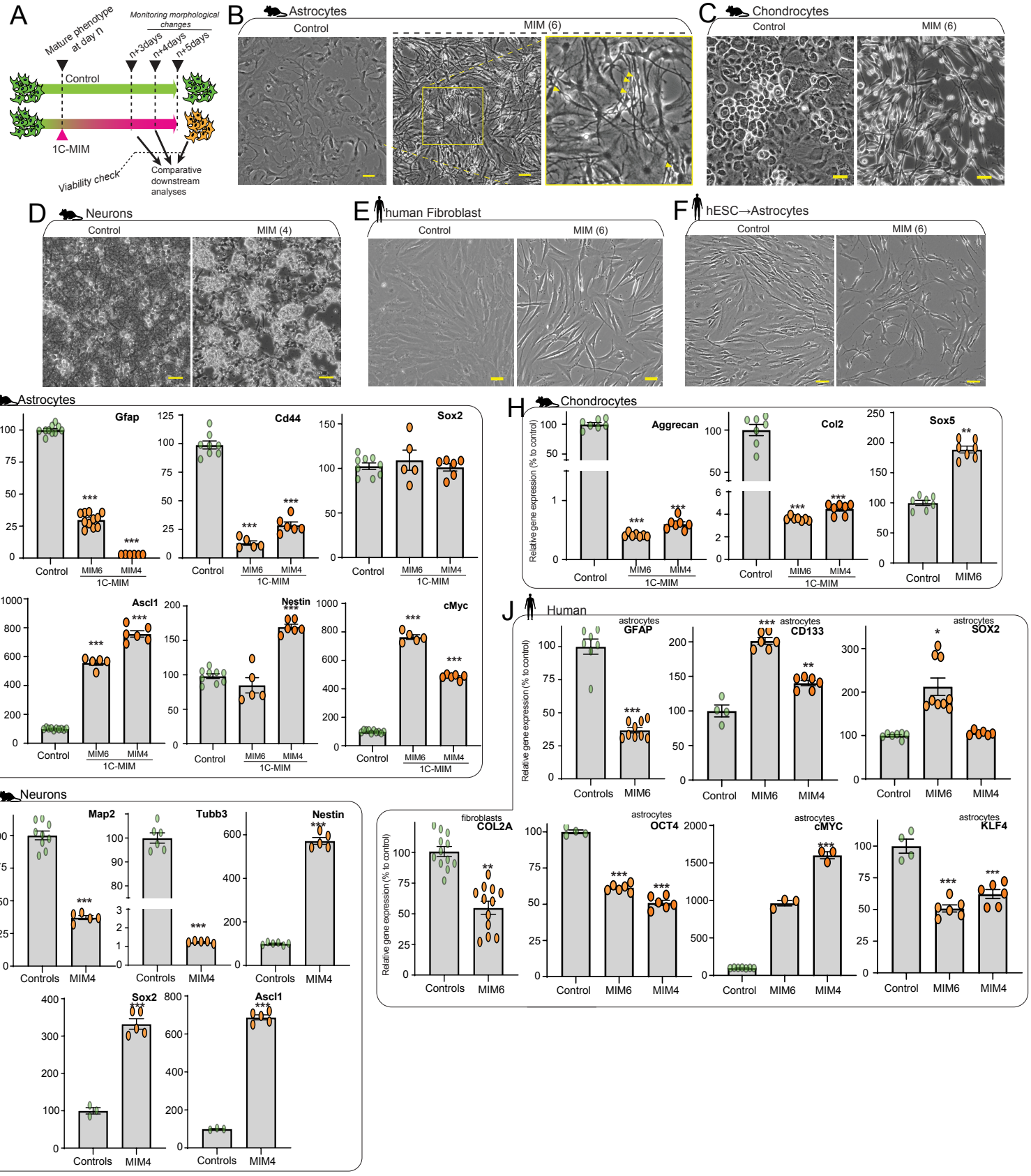

Fig. S4. Basic gene marker screening on differentiated cells treated with 1C-MIM.

(**A**) Experimental setup for supplementation: cells cultured from the same batch are maintained for the time necessary to express mature markers under a differentiation condition (according to each lineage, mature markers expression differs on time, represented in the schema as 'n'). Then cell populations of the same batch are separated and exposed to a control or 1C-MIM-supplemented medium with feeding every other day. MIM6 contains Methionine, Glycine, Putrescine, Cysteine, S-adenosylmethionine; while MIM4 is the former composition minus Cysteine and S-adenosylmethionine. The time for collection was determined in each cell type by observing changes in morphology. For mouse neural-related cells, samples were collected after 4 days of supplementation, for chondrocytes and fibroblasts after 5 days. Note: only muscle cells were collected after 3 days of supplementation (images not presented here, but in the main figure 2). The cell viability was determined at the time of collection as detailed in the Star Methods, and then samples were used for downstream analysis as required.

(**B-F**) Bright-field representative images of cultures of mouse astrocytes, chondrocytes, neurons; and human fibroblasts and astrocytes. Scale bar 50µm. The yellow square in (B) reflects the digital zoom observed in the image located to the right, for details on morphology.

(**G-J**) Representative markers were measured by qRT-PCR in the indicated cell types. The gene expression of genes of interest was normalized with the geometric mean of at least two housekeeping genes (from Actb, Gapdh, and Nat1) and then normalized vs. control conditions. Each dot represents an independent sample (n > 3), where differences compared with control are significant at *P<0.05, **P<0.005, ***P<0.001. Related to Figures 2, 3.

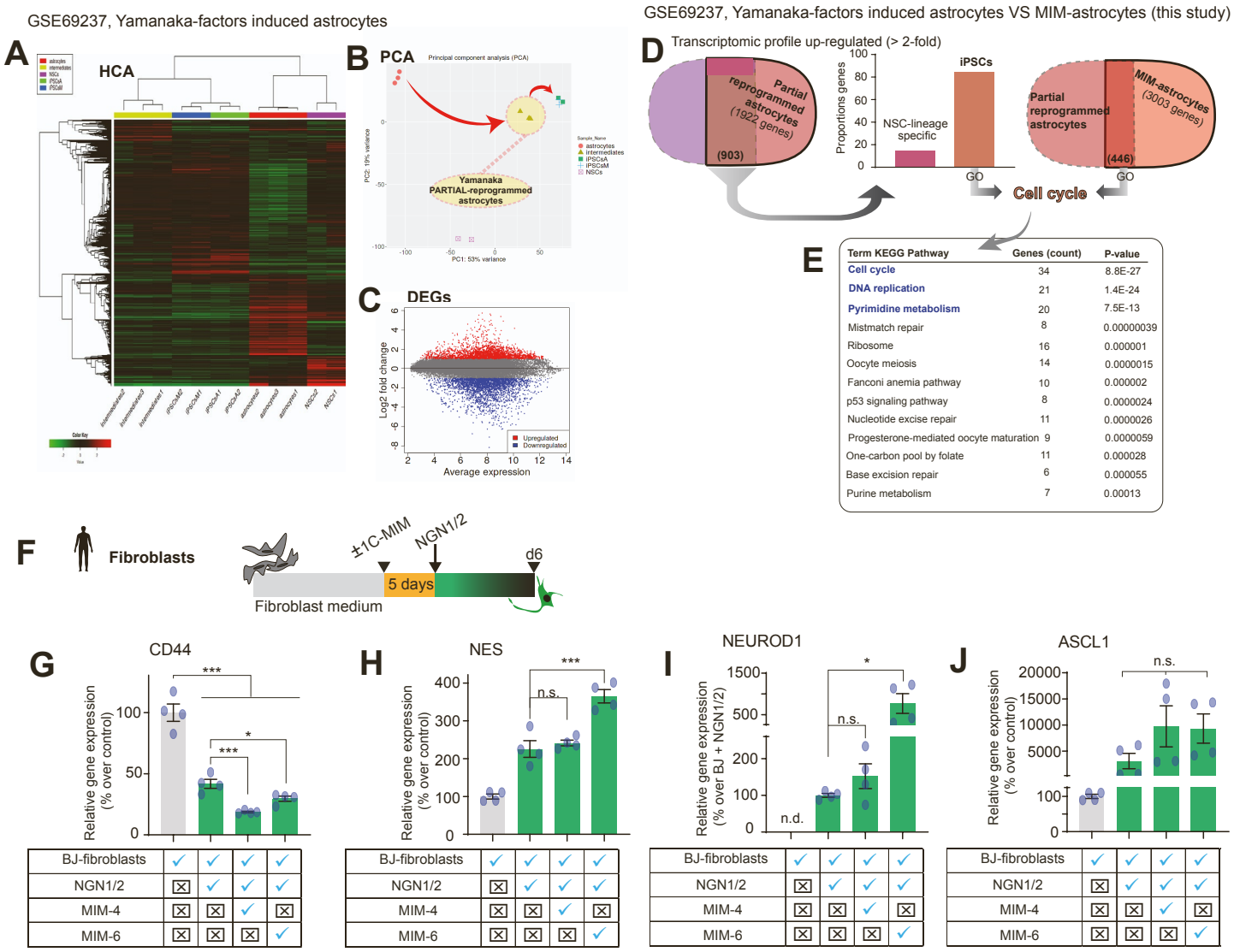

Fig. S5. Orthogonal readouts in astrocytes and fibroblasts corroborate the facilitation of identity transitions by 1C-MIM supplementation in vitro.

(**A-E**) 1C-MIM supplementation induced an intermediate like-progenitor state by regulating cell cycle in astrocytes. In (A) HCA, in (B) PCA, and in (C) volcano plot of DEG. Euclidean distance of RNAseq from astrocytes and intermediate reprogrammed cells (by canonical Yamanaka factors) compared with NSCs and iPSC as reference. The former available database GSE69237 was used to generate these representations. In (**D**) comparison between that former data (GSE69237) and the MIM-astrocytes of this study: where, Venn diagrams show the intersection of the transcriptomic profiles of the indicated populations; and the bars in between represent quantity and type of genes identified in the intersections. Of note 446 genes are shared between partial-reprogrammed and MIM astrocytes; particularly, those genes belong to iPSC-reprogrammed marks and are functionally enriched by Gene Ontology to a cell cycle function as shown in (E).

(**F-J**) Functional assay for the transdifferentiation of human BJ-fibroblasts into neuron-like cells enhanced by 1C-MIM. Schematic representation of the pre-treatment with 1C-MIM before the induction of Neurogenin 1+2 (NGN1/2) in (F). Relative expression of genes for fibroblast-identity in (G) and neuron-identity in (H-J). The expression was normalized with the mean of the housekeeping gene CTCF, then normalized vs. control condition BJ-fibroblasts; except in (l) where NEUROD1 was not detected in fibroblasts and the conditions with MIM were normalized vs. BJ-fibroblast + NGN1/2. Blue dots represent each value ± SEM.

Significantly differences at *P<0.05, **P<0.005, ***P<0.0001. Related to Figure 3.

A

TOTAL mice used in this study	87				
Distribution summary	Control-untreated	1C-MIM-intervention	1C-MIM-intervention-short_term + HIGHdose	Glycine-intervention	Scramble-intervention
	37	30	12	4	4
ROUND 1					
Intervention started at age of 6 weeks-old					
Intervention finished at age of 17.5 weeks-old					
Conditions (MALES strain strain ICR-CD1)	Control-untreated	1C-MIM-intervention			
#mice per condition:	4	5			
ROUND 2					
Intervention started at age of 9 weeks-old					
Intervention finished at age of 22.5 weeks-old					
Conditions (FEMALES, strain ICR-CD1)	Control-untreated	1C-MIM-intervention			
#mice per condition:	3	5			
ROUND 3					
Intervention started at age of 10 weeks-old					
Intervention finished at age of 14.5 weeks-old					
Conditions (BothGenres, strain ICR-CD1)	Control-untreated		Short term +High Dose		
#mice per condition (females):	3		3		
#mice per condition (males);	3		4		
ROUND 4					
Intervention started at age of 9 weeks-old					
Intervention finished at age of 15 weeks-old					
Conditions (MALES, strain ICR-CD1)	Control-untreated	1C-MIM-intervention	Short term +High Dose		
#mice per condition:	10	5	5		
#mice **without injury** per condition:	3	4			
ROUND 5					
Intervention started at age of 9 weeks-old					
Intervention finished at age of 22.5 weeks-old					
Conditions (MALES, strain C57BL/6J)	Control-untreated	1C-MIM-intervention		Gly_intervention	Scr_intervention
#mice per condition :	4	4		4	4
ROUND 6					
Intervention started at age of 72 weeks-old					
Intervention finished at age of 88.5 to 90 weeks-old					
Conditions (MALES, strain C57BL/6J)	Control-untreated	1C-MIM-intervention			
#mice per condition (ended at 88.5wo):	3	3			
#mice per condition (ended at 90wo):	4	4			

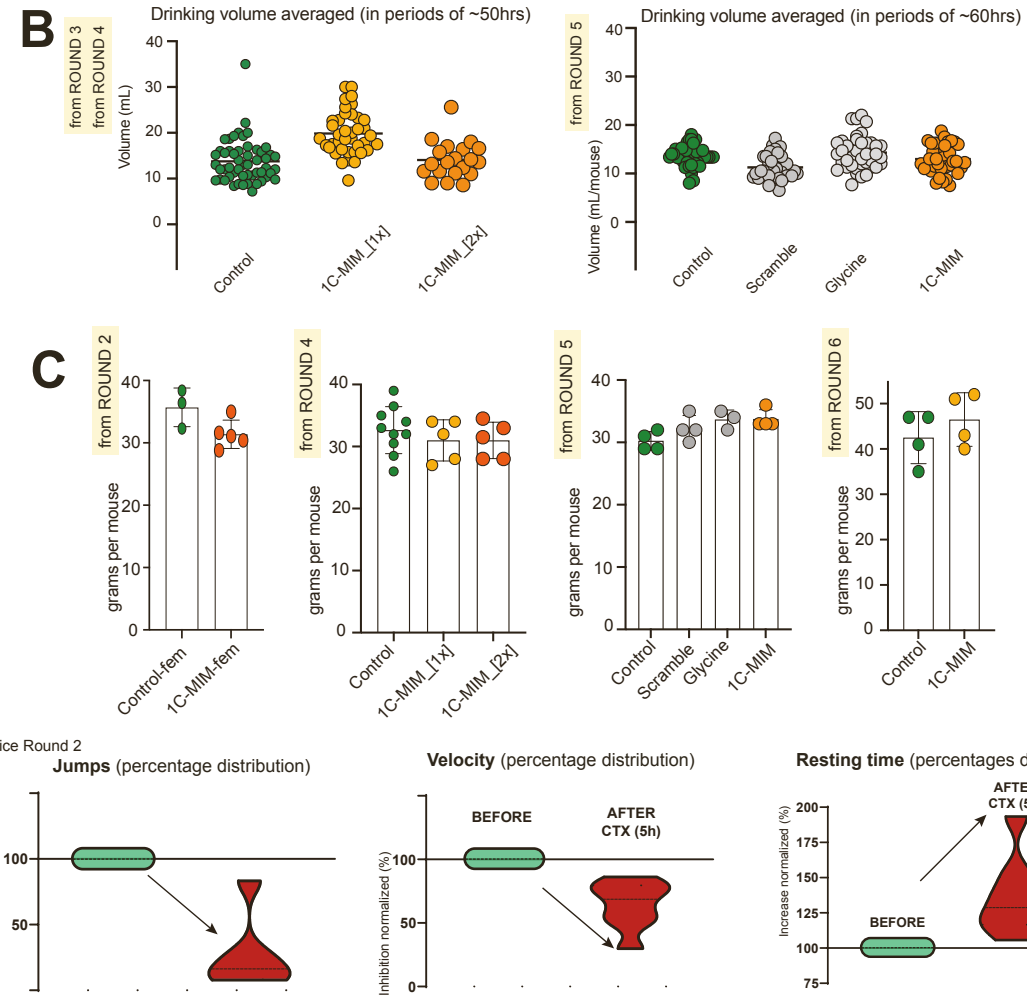

Fig. S6. Experimental design and immediate parameters evaluated for the in vivo intervention with 1C-MIM.
(**A**) Distribution per round of the 87 mice used in the study. Each round represents the experimental intervention used for the study. Only two mice including control and 1C-MIM treated exhibited tumors, and only in the group of aged animals (round 6), therefore no correlation of tumor emergence was associated with the intervention.
(**B**) Drinking volumes. The drinking supplementation was replaced every other day with a standard volume, and measurements of consumption were taken during the intervention. The volumes were normalized according to the number of mice per cage.
(**C**), Bodyweight measurements after 1C-MIM drinking supplementation per round. Each dot represents one mouse.
(**D**) Movement impairment elicited after 5 hours of CTX injection evaluated in terms of jumps, velocity, and resting time. Measurements derived from the Open Field Test, recorded for a period of 60 minutes, graphs represent the distribution including control and 1C-MIM supplemented mice.
Related to Figures 4, 5, 6.

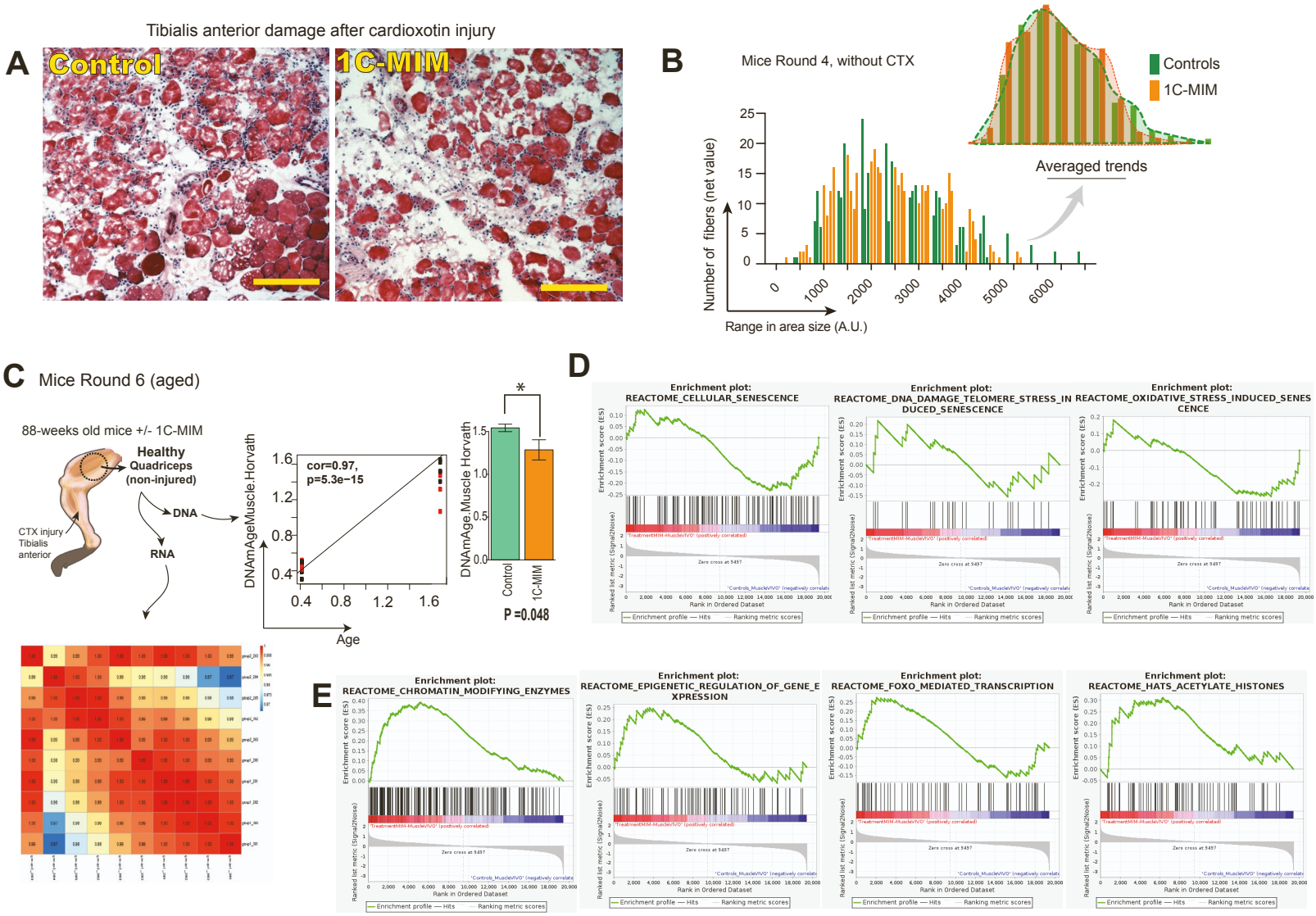

Fig. S7. Analyses on the 1C-MIM intervention in muscle with and without CTX injury.
(**A**) Representative histology images ~5 hours after CTX-injury showing similar damage in control and 1C-MIM supplemented mice. Tibialis anterior sections are stained by H&E (scale bar =250µm).
(**B**) Myofiber size distribution of centrally nucleated fibers without CTX injury of control and 1C-MIM supplemented mice. Insert to the right represents the average.
(**C**) DNA methylation clock using the Horvath Clock demonstrates rejuvenation after 1C-MIM supplementation in quadriceps non-injured. Left panel, schematic representation of how same samples were processed for transcriptomics and methylation, middle correlation analysis; and right panel, estimation of the methylation age using the Horvath clock for muscle. Tissues were recovered at 88-weeks old mice.
(**D-E**) Gene set enrichment analyses from transcriptomic analysis. See also Fig. 6A.

Table S1. Identification of pathways relevant to the intermediate transition (bell pattern). The below pathways represent the enrichments obtained by Metaboanalyst®. Source of the Venn diagram for the intermediate transition.
Experiments were from n=5 biological replicates.
Related to Figure 1G.

MBs, cluster4 (n=194)	NSCs, cluster#3 (n=145)	MSCs, cluster#1 (n=71)
Glycine and Serine Metabolism	Methionine Metabolism	Phosphatidylcholine Biosynthesis
Carnitine Synthesis	Methylhistidine Metabolism	Spermidine and Spermine Biosynthesis
Urea Cycle	Spermidine and Spermine Biosynthesis	Aspartate Metabolism
Glucose-Alanine Cycle	Homocysteine Degradation	Taurine and Hypotaurine Metabolism
Nucleotide Sugars Metabolism	Betaine Metabolism	Phosphatidylethanolamine Biosynthesis
Betaine Metabolism	Taurine and Hypotaurine Metabolism	Phospholipid Biosynthesis
Arginine and Proline Metabolism	Glycine and Serine Metabolism	Arginine and Proline Metabolism
De Novo Triacylglycerol Biosynthesis	Purine Metabolism	Methylhistidine Metabolism
Glutamate Metabolism	Sphingolipid Metabolism	Carnitine Synthesis
Ammonia Recycling	Valine, Leucine and Isoleucine Degradation	Methionine Metabolism
Malate-Aspartate Shuttle	Glutathione Metabolism	Glycolysis
Cardiolipin Biosynthesis	Pantothenate and CoA Biosynthesis	Plasmalogen Synthesis
Plasmalogen Synthesis	Glutamate Metabolism	Urea Cycle
Methionine Metabolism	Carnitine Synthesis	Warburg Effect
Galactose Metabolism	Arginine and Proline Metabolism	Gluconeogenesis
Ketone Body Metabolism	Cysteine Metabolism	Glycine and Serine Metabolism
Glutathione Metabolism	Phosphatidylethanolamine Biosynthesis	Sphingolipid Metabolism
Transfer of Acetyl Groups into Mitochondria	Histidine Metabolism	Beta Oxidation of Very Long Chain Fatty Acids
Phosphatidylcholine Biosynthesis	Selenoamino Acid Metabolism	Mitochondrial Electron Transport Chain
Starch and Sucrose Metabolism	Phosphatidylcholine Biosynthesis	Catecholamine Biosynthesis
Citric Acid Cycle	Ammonia Recycling	Vitamin B6 Metabolism
Beta-Alanine Metabolism	Beta-Alanine Metabolism	Ubiquinone Biosynthesis
Glycerolipid Metabolism	Alanine Metabolism	Purine Metabolism
Glycolysis	Phosphatidylinositol Phosphate Metabolism	Glutathione Metabolism
Aspartate Metabolism	Aspartate Metabolism	Betaine Metabolism
Gluconeogenesis	Nicotinate and Nicotinamide Metabolism	Glutamate Metabolism
Alanine Metabolism	Nucleotide Sugars Metabolism	Estrone Metabolism
Cysteine Metabolism	Catecholamine Biosynthesis	Glycerolipid Metabolism
Homocysteine Degradation	Vitamin B6 Metabolism	Oxidation of Branched Chain Fatty Acids
Mitochondrial Beta-Oxidation of Short...	Ubiquinone Biosynthesis	Mitochondrial Beta-Oxidation of Short...
Warburg Effect	Lactose Synthesis	Phenylalanine and Tyrosine Metabolism
Mitochondrial Beta-Oxidation of Long...	Pyrimidine Metabolism	Mitochondrial Beta-Oxidation of Long...
Pyruvate Metabolism	Transfer of Acetyl Groups into Mitochondria	Starch and Sucrose Metabolism
Pyruvaldehyde Degradation	Estrone Metabolism	Ammonia Recycling
Butyrate Metabolism	Urea Cycle	Citric Acid Cycle
Mitochondrial Electron Transport Chain	Lysine Degradation	Fructose and Mannose Degradation
Ethanol Degradation	Citric Acid Cycle	Amino Sugar Metabolism
Phospholipid Biosynthesis	Fatty Acid Biosynthesis	Nicotinate and Nicotinamide Metabolism
Threonine and 2-Oxobutanoate Degradation	Galactose Metabolism	Tyrosine Metabolism
Glycerol Phosphate Shuttle	Porphyrin Metabolism	Galactose Metabolism
Taurine and Hypotaurine Metabolism	Propanoate Metabolism	Histidine Metabolism
Inositol Metabolism	Pyruvate Metabolism	Fatty acid Metabolism
Methylhistidine Metabolism	Warburg Effect	Pyruvate Metabolism
Caffeine Metabolism	Tryptophan Metabolism	Tryptophan Metabolism
Estrone Metabolism	Bile Acid Biosynthesis	Bile Acid Biosynthesis
Nicotinate and Nicotinamide Metabolism	Tyrosine Metabolism	Arachidonic Acid Metabolism
Phytanic Acid Peroxisomal Oxidation		
Inositol Phosphate Metabolism		
Mitochondrial Beta-Oxidation of Medium...		
Purine Metabolism		

Table S2. Identification of trends of one-carbon metabolites during the intermediate stage between steady-state of Myoblasts (MBs) and early transitional-states of differentiated counterparts. Statistical trends in the relative abundance of individual metabolites at the indicated times. Times selected by their potential overlap with the earliest/immediate transcriptional changes derived from the induction of differentiation. Experiments were from n=5 biological replicates.
Related to Figure 1 and descriptive of Supplemental figure 1D.

PATHWAYS	Comparisons	*Comparison of MBs vs 6 hours of differentiation*	*Comparison of MBs vs 12 hours of differentiation*	*Comparison of MBs at 12 hours of differentiation vs 96 hours differentiation*
Methionine-SAM Metabolism	Significant positive trend (p<0.05)	Cysteine, methionine, cysteine sulfinic acid.	Cysteine, methionine, taurine, homocysteine, cysteine sulfinic acid.	Cysteine-sulfinic acid, SAH, cystine, methionine sulfoxide.
	Positive trend (p<0.10)	Not applicable.	Not applicable.	Not applicable.
	Insignificant change (p>0.1)	SAH, SAM, hypotaurine, N-acetylmethionine, taurine, cystine, homocysteine.	SAH, SAM, cystine, N-acetylcysteine, N-acetylmethionine, N-formylmethionine.	S-methylcysteine, cysteine, S-methylmethionine, S-methylcysteine-sulfoxide, methionine sulfone.
	Negative trend (p<0.10)	N-acetylmethionine sulfoxide.	Hypotaurine, cystathionine.	DMPTA, N-acetylmethionine.
	Significant negative trend (p<0.05)	S-methylcysteine sulfoxide, S-methylmethionine, S-methylcysteine, DMPTA, methionine sulfone, methionine sulfoxide, cystathionine, N-formylmethionine, N-acetylcysteine, N-acetyltaurine.	S-methylcysteine sulfoxide, S-methylmethionine, S-methylcysteine, N-acetyltaurine, methionine sulfoxide, DMPTA, methionine sulfone, N-acetylmethionine sulfoxide.	Methionine, N-formylmethionine, SAM, N-acetylcysteine, hypotaurine, homocysteine, cystathionine, N-acetyltaurine, taurine, N-acetylmethionine-sulfoxide.
Gly-Ser-Thr Metabolism	Significant positive trend (p<0.05)	Threonine, serine, phosphoserine.	Threonine, serine.	Dimethylglycine.
	Positive trend (p<0.10)	Not applicable.	Phosphoserine.	Not applicable.
	Insignificant change (p>0.1)	Glycine	N-acetylthreonine, glycine.	Not applicable.
	Negative trend (p<0.10)	Not applicable.	Not applicable.	Not applicable.
	Significant negative trend (p<0.05)	Dimethylglycine, betaine, N-acetylserine, N-acetylthreonine.	Dimethylglycine, betaine, N-acetylserine.	Threonine, N-acetylserine, serine, betaine, glycine, phosphoserine, N-acetylthreonine.
Polyamine Metabolism	Significant positive trend (p<0.05)	MTA, spermine, spermidine.	MTA, spermine, spermidine.	N-acetylputrescine, putrescine.
	Positive trend (p<0.10)	Not applicable.	Not applicable.	Not applicable
	Insignificant change (p>0.1)	Not applicable.	N-acetylspermidine.	A-acetamidobutanoate.
	Negative trend (p<0.10)	Not applicable.	Not applicable.	Not aplicable.
	Significant negative trend (p<0.05)	4-acetamidobutanoate, N-acetylspermidine, N-acetylisoputreanine, N-acetylputrescine, putrescine.	N-acetyl isoputreanine, 4-acetamidobutanoate, N-acetylputrescine, putrescine.	N-acetyl-isoputreanine, spermine, spermidine, N-acetylspermidine, MTA.
Glutathione Metabolism	Significant positive trend (p<0.05)	Cyclyc dGSH, GSNO, CoA-glutathione, GSSG, S-methylglutathione.	Cyclyc dGSH, GSH, S-nitrosoglutathione, S-methylglutathione, 4-hydroxy-nonenal-glutathione, GSSG,	Cysteine-glutahione disulfide, 5-oxoproline.

CONTINUE TABLE S2

		cysteinglycine, S-lactoylglutathione.	
Positive trend (p<0.10)	Not applicable.	Not applicable.	Not applicable.
Insignificant change (p>0.1)	Cysteine-glutathione disulfide, cysteinglycine, S-lactoylglutathione, 4-hydroxy-nonenal glutathione, glutathione reduced.	Dicarboxylethylglutathione, CoA-glutathione.	CoA-glutathione, 2-hydroxybutyrate.
Negative trend (p<0.10)	Not applicable.	Not applicable.	Not applicable.
Significant negative trend (p<0.05)	Opthalmalate, 5-oxoproline, 2-hydroxybutyrate, dicarboxyethylglutathione.	Opthalmalate, 5-oxoproline, 2-hydroxybutyrate, cysteine-glutathione disulfide.	Opthalmalate, cyclic dGSH, S-lactoylglutathione, dicarboxylethylglutathione, GSSG, GSNO, cysteinglycine, S-methylglutathione, 2-hydroxybutyrate, 4-hydroxy-nonenal-glutathione.

Table S3. Identification of trends of one-carbon metabolites during the intermediate stage between steady-state of Neural Stem Cells (NSCs) and early transitional-states of differentiated counterparts. Statistical trends in the relative abundance of individual metabolites at the indicated times. Times selected by their potential overlap with the earliest/immediate transcriptional changes derived from the induction of differentiation. Experiments were from n=5 biological replicates.
Related to Figure 1 and descriptive of Supplemental figure 1E.

PATHWAYS	Comparisons	*Comparison of NSCs vs 6 hours of differentiation*	*Comparison of NSCs vs 12 hours of differentiation*	*Comparison of NSCs at 12 hours of differentiation vs 72 hours differentiation*
Methionine-SAM Metabolism	Significant positive trend (p<0.05)	SAM, cysteine, methionine, N-acetylcysteine, sulfo-L-alanine, N-acetylmethionine, S-methylcysteine, S-methylcysteine sulfoxide, taurine, N-acetyltaurine, methionine sulfoxide, N-acetylmethionine sulfoxide.	SAM, methionine, cysteine, N-acetylcysteine, N-acetyltaurine, taurine, sulfo-L-alanine, methionine sulfoxide, N-acetylmethionine sulfoxide, N-acetylmethionine, S-methylcysteine-sulfoxide.	SAH, cystathionine, N-acetyltaurine, S-methylcysteine, taurine, methionine sulfone.
	Positive trend (p<0.10)	Not applicable.	S-methylcysteine.	S-methylcysteine sulfoxide.
	Insignificant change (p>0.1)	SAH, cysteine sulfinic acid.	SAH, cysteine sulfinic acid.	Methionine sulfoxide, methionine.
	Negative trend (p<0.10)	Not applicable.	Not applicable.	Not applicable.
	Significant negative trend (p<0.05)	Cystathionine, hypotaurine, N-formylmethionine.	Cystathionine, hypotaurine, N-formylmethionine.	N-formylmethionine, hypotaurine, cysteine, SAM, N-acetylcysteine, sulfo-L-alanine, N-acetylmethionine, cysteine sulfinic acid.
Gly-Ser-Thr Metabolism	Significant positive trend (p<0.05)	Threonine, glycine, betaine, serine, dimethylglycine, homoserinelactone, N-acetylglycine.	Betaine, glycine, serine, dimethylglycine, homoserinelactone, N-acetylglycine.	N-acetylserine, betaine, dimethylglycine, N-acetylglycine.
	Positive trend (p<0.10)	N-acetylserine.	Not applicable.	N-acetylthreonine.
	Insignificant change (p>0.1)	Phosphothreonine.	Threonine, phosphothreonine, N-acetylserine.	Threonine.
	Negative trend (p<0.10)	Not applicable.	Not applicable.	Phosphothreonine.
	Significant negative trend (p<0.05)	N-acetylthreonine.	N-acetylthreonine.	Glycine, serine, homoserinelactone.
Polyamine Metabolism	Significant positive trend (p<0.05)	Putrescine, MTA, N-acetylputrescine, 4-acetamidobutanoeate.	Putrescine, MTA, N-acetylputrescine, 4-acetamidobutanoeate.	4-acetamidobutanoate.
	Positive trend (p<0.10)	Not applicable.	Not applicable.	Not applicable.
	Insignificant change (p>0.1)	N-acetylspermidine, N-diacetylspermine.	N-acetylspermidine, N-diacetylspermine.	N-acetylspermidine.
	Negative trend (p<0.10)	Not applicable.	Not applicable.	Not applicable.

	Significant negative trend (p<0.05)	Spermidine.	Spermidine.	Putrescine, spermidine, MTA, M-acetylputrescine, N-diacetylspermine.
Glutathione Metabolism	Significant positive trend (p<0.05)	2-hydroxybutyrate, GSSG, cysteine-glutathine disulfide, opthalmalate.	2-hydroxybutyrate, GSSG, opthalmalate, cysteine-glutathione disulfide.	2-hydroxybutyrate, 5-oxoproline, 4-hydroxynonenal-glutathione.
	Positive trend (p<0.10)	Not applicable.	Not applicable.	Not applicable.
	Insignificant change (p>0.1)	4-hydroxy-nonenal glutathione.	4-hydroxy-nonenal-glutathione.	Cysteine-glutathione disulfide, cysteinglycine.
	Negative trend (p<0.10)	Not applicable.	Not applicable.	Not applicable.
	Significant negative trend (p<0.05)	GSH, S-lactoylglutathione, S-methylglutathione, cysteinglycine, 5-oxoproline.	S-lactoylglutathione, S-methylglutathione, 5-oxoproline, GSH, cysteinglycine.	S-lactoylglutathione, GSSG, S-methylglutathione, GSH, opthalmalate.

Table S4. Identification of trends of one-carbon metabolites during the intermediate stage between steady-state of Mesenchymal Stem Cells (MSCs) and early transitional-states of differentiated counterparts. Statistical trends in the relative abundance of individual metabolites at the indicated times. Times selected by their potential overlap with the earliest/immediate transcriptional changes derived from the induction of differentiation. Experiments were from n=5 biological replicates.
Related to Figure 1 and descriptive of Supplemental figure 1F.

PATHWAYS	Comparisons	*Comparison of MSCs vs 6 hours of differentiation*	*Comparison of MSCs vs 24 hours of differentiation*	*Comparison of MSCs at 24 hours of differentiation vs 96 hours differentiation*
Methionine-SAM Metabolism	Significant positive trend (p<0.05)	Methionine, cysteine s-sulfate, SAM, taurine, methionine sulfoxide, hypotaurine, N-acetylmethionine sulfoxide.	Methionine, N-acetyltaurine, cystine, cysteine sulfinic acid, methionine sulfoxide.	Cystine, cysteine s-sulfate, methionine sulfoxide.
	Positive trend (p<0.10)	S-methylcysteine.	Cysteine s-sulfate.	Not applicable.
	Insignificant change (p>0.1)	SAH, cystine, cysteine sulfinic acid.	SAM, cysteine, taurine, hypotaurine.	SAM, methionine, DMPTA, N-acetylmethionine sulfoxide, S-methylcysteine, cysteine sulfinic acid, N-formylmethionine.
	Negative trend (p<0.10)	Not applicable.	N-formylmethionine.	N-acetylmethionine.
	Significant negative trend (p<0.05)	N-acetylmethionine, N-acetylcysteine, methionine sulfone, cysteine, N-acetyltaurine, DMPTA, N-formylmethionine.	N-acetylmethionine, N-acetylcysteine, DMPTA, S-methylcysteine, methionine sulfone, SAH, N-acetylmethionine sulfoxide.	N-acetylcysteine, methionine sulfone, cysteine, SAH, taurine, N-acetyltaurine, hypotaurine.
Gly-Ser-Thr Metabolism	Significant positive trend (p<0.05)	Threonine, N-acetylthreonine.	Threonine, N-acetylthreonine, glycine, serine, N-acetylserine.	N-acetylthreonine.
	Positive trend (p<0.10)	Glycine, serine.	Not applicable.	Not applicable.
	Insignificant change (p>0.1)	N-acetylserine.	Not applicable.	Threonine, Serine.
	Negative trend (p<0.10)	Not applicable.	Not applicable.	Not applicable.
	Significant negative trend (p<0.05)	Betaine, dimethylglycine.	Betaine, dimethylglycine.	Betaine, dimethylglycine, glycine, N-acetylserine.
Polyamine Metabolism	Significant positive trend (p<0.05)	MTA.	Putrescine, N-acetylspermidine.	Not applicable.
	Positive trend (p<0.10)	Not applicable.	N-acetylputrescine.	Not applicable.
	Insignificant change (p>0.1)	N-acetylspermidine, N-acetylputrescine, putrescine, spermine, spermidine.	Spermidine, Spermine.	Spermine, N-acetylputrescine, 4-acetamidobutanoate.
	Negative trend (p<0.10)	Not applicable.	MTA.	Not applicable.
	Significant negative trend (p<0.05)	4-acetamidobutanoeate.	4-acetamidobutanoeate.	Spermidine, N-acetylspermidine, MTA, putrescine.
Glutathione Metabolism	Significant positive trend (p<0.05)	CoA-glutathione, GSSG, 4-hydroxy-nonenal-glutathione, S-methylglutathione.	Cysteine glutathione-disulfide.	5-oxoproline.
	Positive trend (p<0.10)	Dicarboxyethylglutathione, cysteine glutathione-disulfide.	Not applicable.	Not applicable.
	Insignificant change (p>0.1)	Cysteinglycine, GSH, S-lactoylglutathione, 3-dephospho-CoA-glutathione.	Cysteinglycine, 5-oxoproline, S-lactoylglutathione.	CoA-glutathione, 3-dephospho-CoA-glutathione, 4-hydroxy-nonenal-glutathione, S-

CONTINUE TABLE S4

			methylglutathione, GSH, S-lactoylglutathione, dicarboxyethylglutathione.
Negative trend (p<0.10)	Not applicable.	Not applicable.	2-hydroxybutyrate.
Significant negative trend (p<0.05)	Ophtalmate, 5-oxoproline, 2-hydroxybutyrate.	Ophtalmate, CoA-glutathione, S-methylglutathione, 2-hydroxybutyrate, dicarboxyethyl glutathione, GSH, GSSG, 4-hydroxy-nonenal-glutathione, 3-dephospho-CoA-glutathione.	Ophtalmate, cysteinglycine, cysteine glutathione-disulfide, GSSG.

Table S5. Sequences of primers, where M for mouse, H for human.
Related to STAR Methods.

Gene name	Specie	Forward primer seq	Revers primer seq
Beta-Actin	M	CATTGCTGACAGGATGCAGAAGG	TGCTGGAAGGTGGACAGTGAGG
Gapdh	M	CATCACTGCCACCCAGAAGACTG	ATGCCAGTGAGCTTCCCGTTCAG
Nat1	M	ATTCTTCGTTGTCAAGCCGCCAAAGTGGAG	AGTTGTTTGCTGCGGAGTTGTCATCTCGTC
RPL38	M	AGGATGCCAAGTCTGTCAAGA	TCCTTGTCTGTGATAACCAGG
Ascl1	M	CTCGTCCTACTCCTCCGACG	ATCTGCTGCCATCCTGCTTC
Cd44	M	ACAACCCTTCAGCCTACTGC	CGCCGCTCTTAGTGCTAGAT
Cd9	M	CTGTGGCATAGCTGGTCCTTTG	AGACCTCACTGATGGCTTCAGG
cMyc	M	GTGCTGCATGAGGAGACACC	GACCTCTTGGCAGGGGTTTG
Klf4	M	GCACACCTGCGAACTCACAC	CCGTCCCAGTCACAGTGGTAA
Gfap	M	AGGTTGAATCGCTGGAGGAG	GCTTGGCCACATCCATCTC
Nes	M	CCAGAGCTGGACTGGAACTC	ACCTGCCTCTTTTGGTTCCT
Cd133	M	TCCCTCCTGTGCAGCAATCA	CCAAACTTCTTCGTTTCCCCGA
Sox2	M	AACGGCAGCTACAGCATGATGC	CGAGCTGGTCATGGAGTTGTAC
Hes5	M	CCGTCAGCTACCTGAAACACAG	GGTCAGGAACTGTACCGCCTC
Mtr	M	GCTCTGTGAAGACCTCATCTGG	GAGCCATTCCTCCACTCATCTG
Chrd1	M	GTATGCAGAGGGGATGCAGAA	TGGAGGATCGTAGGGGGAAC
Odc1	M	TGCCACACTCAAAACCAGCAGG	ACACTGCCTGAACGAAGGTCTC
Beta-III-tubulin	M	ACCTATTCAGGCCCGACAACTTTA	GCAGGCAGTCACAATTCTCACAC
Map2	M	CTGCGAGTAAGCTGTGACCG	AGCTGAGGAACCTTAATTCTTGCC
SB100	M	GACTCCAGCAGCAAAGGTGA	TGATTTCCTCCAGGAAGTGAGAG
Mat1a	M	CCTTCTCTGGAAAGGACTACACC	GACAGAGGTTCTGCCACACCAA
Ascl1	M	CGGAACTGATGCGCTGCAAACG	GGCAAAACCCAGGTTGACCAAC
Sox5	M	CGCCAGATGAAAGAGCAACTCAG	TGAGTCAGGCTCTCCAGTGTTG
Cd51	M	GTGTGAGGAACTGGTCGCCTAT	CCGTTCTCTGGTCCAACCGATA
Thy1	M	CCTTACCCTAGCCAACTTCACC	TTATGCCGCCACACTTGACCAG
Sox9	M	GCAGACCAGTACCCGCATCT	CTCGTTCAGCAGCCTCCAG
Aggrecan	M	CCTGCTACTTCATCGACCCC	AGATGCTGTTGACTCGAACCT
Col2a	M	AATGGGCAGAGGTATAAAGATAAGGA	CATTCCCAGTGTCACACACACA
Myf5	M	GGTGGAGAACTATTACAGCCTGC	ACAGTAGATGCTGTCAAAGCTGC
Ccnd1	M	GCAGAAGGAGATTGTGCCATCC	AGGAAGCGGTCCAGGTAGTTCA
Gdf6	M	CACTAGCTTTGTAGACAGAGGAC	CCTGGCGATAAAGCCTTAGCTC
Myh11	M	GCAACTACAGGCTGAGAGGAAG	TCAGCCGTGACCTTCTCTAGCT
Cldn2	M	AGGACTTCCTGCTGACATCCAG	AATCCTGGCAGAACACGGTGCA
Ckm	M	GGCTTCACTCTGGACGATGTCA	CCTTGAAGACCGTGTAGGACTC
Mef2c	M	GTGGTTTCCGTAGCAACTCCTAC	GGCAGTGTTGAAGCCAGACAGA
Vimentin	M	CGGAAAGTGGAATCCTTGCAGG	AGCAGTGAGGTCAGGCTTGGAA
Glast	M	GCGATTGGTCGCGGTGATAATG	CGACAATGACTGTCACGGTGTAC
Glutamine synthetase	M	CTGCCATACCAACTTCAGCACC	CTGGTGCCTCTTGCTCAGTTTG
Myelin Binding Protein	M	TCTGGCAAGGACTCACACAC	AGGTGGTGTTCGAGGTGTCA
O4	M	TGTAACAGGTCCTCGGAAGGG	TGTGCAAGGACAGGTTGTGAC
NSE	M	TGGCAAGGATGCCACTAACGTG	AACTCAGAGGCAGCCACATCCA
Synaptophysin	M	TTGGCTTCGTGAAGGTGCTGCA	ACTCTCCGTCTTGTTGGCACAC
CTCF	H	GGGCTTGAGAGCTGGGTTCTATT	CTTCGACTGCATCACCTTCCATT
NESTIN	H	GCACCTCAAGATGTCCCTCAGC	GTTTGCAGCCGGGAGTTCTCA
NEUROD1	H	TCACTGCTCAGGACCTACTAACAACA	GTCTGTCCAGCTTGGAGGACCTT
ASCL1	H	CGACTTCACCAACTGGTTCTGAG	TAAAGATGCAGGTTGTGCGATCA
CD44	H	CCAGAAGGAACAGTGGTTTGGC	ACTGTCCTCTGGGCTTGGTGTT
GUS B	H	GGTTTCACCAGGATCCACCTC	ACTCTCGTCGGTGACTGTTC
GAPDH	H	AATCCCATCACCATCTTCCA	TGGACTCCACGACGTACTCA
SOX2	H	CAAAAATGGCCATGCAGGTT	AGTTGGGATCGAACAAAAGCTATT
GFAP	H	AGAGATCCGCACGCAGTATG	GTAGTCGTTGGCTTCGTGCT
cMYC	H	GGATTCTCTGCTCTCCTCGAC	AGACTCTGACCTTTTGCCAGG

CONTINUE TABLE S5

CD133	H	CACTACCAAGGACAAGGCGTTC	CAACGCCTCTTTGGTCTCCTTG
OCT4	H	CCTGAAGCAGAAGAGGATCACC	AAAGCGGCAGATGGTCGTTTGG
KLF4	H	CATCTCAAGGCACACCTGCGAA	TCGGTCGCATTTTTGGCACTGG
NANOG	H	AAATACCTCAGCCTCCAGCAG	CCATTGCTATTCTTCGGCCAG
COL1A2	H	GGCCCTCAAGGTTTCCAAGG	CACCCTGTGGTCCAACAACTC